Original Article

Molecular profiling of gene fusions in soft tissue sarcomas by Ion AmpliSeq™: a study of 35 cases

Rong Wei[1#], Feng Gao[2#], Zixin Zeng[1], Ziwei Gui[1], Yangwei Shang[1], Ningning Shen[1], Ziyue Wang[1], Weixia Han[1], Honghong Shen[1], Xin Li[1], Li E[1], Wenxia Ma[1], Chen Wang[1]

[1]Department of Pathology, Second Hospital of Shanxi Medical University, Taiyuan, China; [2]Department of Orthopedics, Sixth Clinical Medical College, Shanxi Medical University, Taiyuan, China

Contributions: (I) Conception and design: R Wei, F Gao, W Ma, C Wang; (II) Administrative support: W Ma, C Wang; (III) Provision of study materials or patients: Z Zeng, Z Gui, Y Shang, N Shen; (IV) Collection and assembly of data: R Wei, F Gao; (V) Data analysis and interpretation: Z Wang, W Han, H Shen, X Li, L E; (VI) Manuscript writing: All authors; (VII) Final approval of manuscript: All authors.

[#]These authors contributed equally to this work.

Correspondence to: Wenxia Ma; Chen Wang. The Second Hospital of Shanxi Medical University, No. 382 Wuyi Road, Taiyuan 030000, China. Email: mawenxia@sxmu.edu.cn; wangchen@sxmu.edu.cn.

Background: The accurate diagnosis of sarcoma can be difficult as there are over 70 different subtypes. While molecular profiling in soft tissue sarcoma (STS) has gradually been incorporated into routine diagnostics, conventional methods such as fluorescence in situ hybridization (FISH), reverse transcriptase-PCR (RT-PCR), and Sanger sequencing have several drawbacks. By allowing simultaneous analysis of multiple targets and increasing sequencing depth to achieve ultra-sensitivity, next-generation sequencing (NGS) can not only detect common genetic abnormalities without prior assumptions but also identify uncommon or even new variants.

Methods: In this study, the applicability of NGS in assessing STS using the Ion Torrent Proton was evaluated and compared with other methods. A cohort of 35 tissue specimens from STS patients, including alveolar soft-part sarcoma (ASPS), Ewing's sarcoma (ES), synovial sarcoma (SS), dermatofibrosarcoma protuberans (DFSP), and myxoid liposarcoma (MLPS) patients, were subjected to NGS by an Ion AmpliSeqTM Custom panel.

Results: A proportion of 97.14% (34/35) were successfully conducted to detect gene fusion positive events and met all criteria for good quality. The concordance between NGS and conventional techniques was 94.12% (32/34). NGS also showed superior results, as Sanger sequencing and FISH in two cases were false negatives, demonstrating the excellent diagnostic utility of NGS for translocation detection in STS.

Conclusions: The results in this study show the potential for NGS to aid in diagnosis and clinical monitoring of STS and warrant additional studies in larger cohorts.

Keywords: Soft tissue sarcoma (STS); molecular profiling; fluorescence in situ hybridization (FISH); next generation sequencing; gene fusion

Submitted Dec 03, 2021. Accepted for publication Mar 14, 2022.
doi: 10.21037/tcr-22-70
View this article at: https://dx.doi.org/10.21037/tcr-22-70

Introduction

Soft tissue sarcoma (STS) represents a heterogeneous group of rare tumors derived from mesenchymal tissue that occur in fat, fascia, muscle, fiber, lymph, blood vessels, and joints (1). Over 70 different histological subtypes of STS have been identified, which brings great difficulties to diagnosis because of the similar pathological manifestations and disordered imaging distributions (2). In addition, some STSs are easily misdiagnosed as benign tumors because of their small size, superficial location, clear borders, and slow

growth (1). These diagnostic errors may lead to mistakes in treatment and a poor prognosis. For example, if a diagnosis is made based on simple clinical palpation and B-ultrasound examination, the STS may be mistakenly regarded as a benign tumor leading to hasty operation, and the lesion may not be identified as an STS until recurrence.

STS has an incidence rate of 5 cases per 100,000 people per year as reported by the World Health Organization (WHO) (3) and are the second most prevalent form of solid tumors and an important group of secondary malignancies, despite accounting for only 1% of all human malignancies (4). Early detection of STS improves the ability to effectively treat these tumors, and the best time for treatment is the first operation. Therefore, the first diagnosis is directly related to the patient's ability to retain function of the involved limb (1). While traditionally, STS is classified according to the morphological appearance and type of the tumor tissue. with the development of molecular pathology, genetic profiling of STS has not only helped to understand its pathogenesis but has improved the accuracy of pathological subtyping (5). Genetic profiling can also be used for prognosis, staging, and monitoring the effect of treatment (6-11).

Gene fusions, a chromosomal rearrangement that causes the juxtaposition of two previously independent coding or regulatory sequences, are present in approximately one-third of all STS cases (1). The strong association between the type of gene fusions and the morphological subtype of STS makes gene fusions an incredibly useful diagnostic marker. The National Comprehensive Cancer Network (NCCN) and the WHO have recommended gene fusions as an auxiliary diagnostic indicator for STS (12,13). Most gene fusions are currently identified by fluorescence *in situ* hybridization (FISH), immunohistochemistry (IHC), or reverse transcription-polymerase chain reaction (RT-PCR)-based Sanger sequencing. However, these methods have low sensitivity and throughput, can detect only one fusion subtype at a time and, can only examine previously identified gene fusions. Currently, the gold standard method for gene fusion detection is FISH and while highly sensitive and specific, it is also labour intensive, subjective in analysis, and unable to screen a large number of gene fusions. In contrast, next-generation sequencing (NGS) not only enables parallel high-throughput sequencing of multiple genes and multiple samples, but also achieves ultra-high detection sensitivity through deep sequencing (14).

In this study, we investigated the applicability of Ion AmpliSeq™ Custom panel NGS on the Ion AmpliSeq Designer (https://www.ampliseq.com/login/login.action) for profiling gene fusions in 35 STS samples. Moreover, we compared the results of NGS with those of FISH, RT-PCR Sanger sequencing, and IHC. We present the following article in accordance with the MDAR reporting checklist (available at https://tcr.amegroups.com/article/view/10.21037/tcr-22-70/rc).

Methods

Sample collection

The retrospective cohort consisted of 35 patients with a confirmed STS diagnosis during the period of 2013 until 2019 in the Second Hospital of Shanxi Medical University, whose formalin-fixed paraffin-embedded (FFPE) tumor tissue samples were retrieved from pathology archives. We retrieved clinical information of patients including age, sex, tumor site, tumor size, and histologic diagnoses. The study protocol was approved by the ethics committees of the Second Hospital of Shanxi Medical University [(2021)YX No. 019], and written informed consent was obtained from all patients prior to the study. The study was conducted in accordance with the Declaration of Helsinki (as revised in 2013).

Nucleic acid isolation

Nucleic acid was isolated from samples using the Magen Hipure FFPE DNA/RNA Kit (Magen, China) and after treatment with DNase, RNA samples were quantified using a Qubit 3.0 Fluorometer (Thermo Fisher Scientific, Carlsbad, CA, USA).

IHC and FISH analysis

Immunohistochemical staining was performed by standard protocols. The FISH was performed on the deparaffinized and ethanol dehydrated 5-μm FFPE slides according to the manufacturer's instruction. The commercially obtained break-apart probes DNA damage inducible transcript 3 (DDIT3) Break Apart, synaptotagmin (SYT) Break Apart, and collagen 1A1 (COL1A1)-platelets-derived growth factor β (PDGFB) (Zytovision, Germany) were used to detect translocations. Slides were counterstained with DAPI before visualization by fluorescence microscopy.

Table 1 Primers for the most common fusion transcripts in STS by reverse transcriptase-PCR

Target	Primer (5' to 3')
COL1A1-E19F1	GGTGCTGTTGGTGCTAAG
COL1A1-E19F2	CAATGGTGCTCCTGGTATT
COL1A1-E32F1	GTGTTCCTGGAGACCTTG
COL1A1-E32F2	AAGAGGCGAGAGAGGTTT
COL1A1-E40F1	GTCCTGGTGAAGTTGGTC
COL1A1-E40F2	TCAAGGTATTGCTGGACAG
PDGFB-E2R2	TGGTCACTCAGCATCTCA
PDGFB-E2R1	AGGCGTTGGAGATCATCA
ASPSCR1-E7F	AAGCCAAAGAAGTCCAAGT
TFE3-E6R	CACGCCTTGACTACTGTA
SS18-E10F	GGTCCAGGTCCTCAGTAT
SSX1-E7R	CAGTTGTTTCCCATCGTTT
SSX2-E6R	CTTCTCAGAGGTAGTTGGTT
SSX4-E6R	CTCTGGCACTTCCTTCAA
FUS-E5F	TATGGTGGACAGCAGCAA
DDIT3-E2R	AGGTGTGGTGATGTATGAAG
FUS-E6F	GCAGTGGTGGCTATGAAC
EWSR1-E7F	GCCAAGCTCCAAGTCAAT
FLI1-E7R	CGTTGCTCTGTATTCTTACTG
ERG-E10R	ATCCGTCATCTTGAACTCC
TFE3-E5R	CTGAGCATTTCATCATTGT
FUS-E7F	GGTTACAACCGCAGCAGT
FLI1-E6R	ATGTTATTGCCCCAAGCTC
SSX1-E6R	CTTCTGACACTCCCTTCGA

ASPSCR1, alveolar soft part sarcoma critical region-1; *COL1A1*, collagen 1A1; *DDIT3*, DNA damage inducible transcript 3; *ERG*, ETS transcription factor; *EWSR1*, Ewing sarcoma breakpoint region 1 gene; *FLI1*, Fli-1 proto-oncogene; *FUS*, FUS RNA binding protein; *PDGFB*, platelets-derived growth factor β; *SS18*, synovial sarcoma translocation chromosome 18; *SSX*, Synovial Sarcoma/X breakpoint; STS, soft tissue sarcoma; *TFE3*, transcription factor binding to IGHM enhancer 3.

RT-PCR and Sanger sequencing

RNA was reverse transcribed by a SuperScript VILO cDNA synthesis kit (Invitrogen, MA, USA), and the synthesized cDNA was subjected to PCR using the Multiplex PCR MasterMix (UNG) according to the manufacturer's protocol. Primers for the detection of the most common fusion transcripts in STS are described in *Table 1* (1). Thermocycling conditions were modified based on previously published methods (14), and the bidirectional Sanger sequencing of the PCR products was conducted on an ABI 3730XL (Thermo Fisher Scientific).

Ion torrent library preparation and sequencing

Approximately 100 ng of RNA was reverse transcribed into cDNA using SuperScript IV VILO Master Mix (Life Technologies, CA, USA). Library preparation was processed with AmpliSeq Assay (Ion AmpliSeq™ Custom panels, IAD187473, and WG_IAD 186692 were designed by Tongshu Biotechnology Co., Changzhou, Jiangsu, China) according to the manufacturer's protocol. The library concentrations were determined by a Qubit 2.0 Fluorometer (Thermo Fisher Scientific) and the normalized RNA libraries were pooled together for loading on Ion P1 chips, followed by sequencing on an Ion Torrent Proton using HiQ chemistry (Life Technologies).

Data analysis

The Torrent Suite™ Browser was used to perform initial quality control on chip loading density and mapped reads number, and qualified sequencing data was further used to identify gene fusions by Ion Reporter™ version 5.0 with standard settings. Manual evaluation was conducted on the sequence accumulation of variants to ensure there was no misreading.

Statistical analysis

SPSS software (version 25.0) was used for all statistical analyses. All statistical tests were two-sided at the 5% level of significance.

Results

General characterization of samples

The 35 STS samples were obtained from 23 male patients, 11 female patients, and 1 patient of unknown sex (the clinical information from this patient was missing). The mean age of patients was 36 years old (range, 14–82 years old, *Table 2*). Histologic differential diagnosis of all cases was confirmed by an experienced pathologist, with the

Table 2 Gene fusions identified by NGS solid fusion assay with Sanger/FISH results

Case	Age (years)	Sex	Diagnosis	Left partner gene	Break point 1	Right partner gene	Break point 2	Sanger/FISH
1	25	M	ASPS	*ASPSCR1*	E7	*TFE3*	E5	C
2	25	M	ASPS	*ASPSCR1*	E7	*TFE3*	E5	C
3	34	M	ASPS	*ASPSCR1*	E7	*TFE3*	E5	C
4	49	M	MLPS	*COL1A1*	E40	*PDGFB*	E2	C
5	47	F	MLPS	*FUS*	E7	*DDIT3*	E2	C
6	42	M	MLPS	*FUS*	E5	*DDIT3*	E2	C
7	82	M	MLPS	*COL1A1*	E19	*PDGFB*	E2	C
8	NP	NP	MLPS	*FUS*	E8	*DDIT3*	E2	C
				COL1A1	E19	*PDGFB*	E2	
9	16	F	ASPS	*ASPSCR1*	E7	*TFE3*	E6	C
10	26	F	ASPS	*ASPSCR1*	E7	*TFE3*	E6	C
11	33	M	ASPS	*ASPSCR1*	E7	*TFE3*	E5	C
12	33	M	ASPS	*ASPSCR1*	E7	*TFE3*	E5	C
13	23	F	ASPS	*COL1A1*	E32	*PDGFB*	E2	C
				ASPSCR1	E7	*TFE3*	E6	
14	60	M	DFSP	*COL1A1*	E38/40/41/42/43	*PDGFB*	E2	C
15	23	M	DFSP	*COL1A1*	E32	*PDGFB*	E2	C
16	28	F	DFSP	*COL1A1*	E39/40/43	*PDGFB*	E2	C
17	28	F	DFSP	*COL1A1*	E34/38/39/40/43	*PDGFB*	E2	C
18	20	M	DFSP	*NA*	NA	*NA*	NA	NA
19	48	F	DFSP	*COL1A1*	E16/19/20	*PDGFB*	E2	C
20	27	M	DFSP	*COL1A1*	E8/37/38/42/43/47	*PDGFB*	E2	C
21	26	M	ES	*EWSR1*	E7	*FLI1*	E6	C
				COL1A1	E32	*PDGFB*	E2	D
22	22	F	ES	*COL1A1*	E40	*PDGFB*	E2	C
				EWSR1	E7	*FLI1*	E6	
23	14	F	ES	*EWSR1*	E7	*ERG*	E10	C
24	17	M	ES	*EWSR1*	E7	*FLI1*	E6	C
25	39	M	SS	*SS18*	E10	*SSX1*	E6	C
26	36	M	SS	*SS18*	E10	*SSX1*	E6	C
				SS18	E10	*SSX4*	E6/7	
27	29	M	SS	*SS18*	E10	*SSX1*	E6	C
				COL1A1	E32	*PDGFB*	E2	D
28	60	M	SS	*SS18*	E10	*SSX1*	E6	C
29	60	M	SS	*SS18*	E10	*SSX1*	E6	C

Table 2 (*continued*)

Table 2 (*continued*)

Case	Age (years)	Sex	Diagnosis	Left partner gene	Break point 1	Right partner gene	Break point 2	Sanger/FISH
30	39	M	SS	*SS18*	E10	*SSX1*	E6	C
31	32	F	DFSP	*COL1A1*	E32/39/44/46/47	*PDGFB*	E2	C
32	42	F	DFSP	*COL1A1*	E32	*PDGFB*	E2	C
33	55	M	DFSP	*COL1A1*	E8/27/30/31/32	*PDGFB*	E2	C
34	46	M	SS	*SS18*	E10	*SSX1*	E6	C
35	38	M	SS	*SS18*	E10	*SSX1*	E6	C

ASPS, alveolar soft-part sarcoma; *ASPSCR1*, alveolar soft part sarcoma critical region-1; C, concordant; *COL1A1*, collagen 1A1; D, discordant; *DDIT3*, DNA damage inducible transcript 3; DFSP, dermatofibrosarcoma protuberans; *ERG*, ETS transcription factor; ES, Ewing's sarcoma; *EWSR1*, Ewing sarcoma breakpoint region 1 gene; F, female; FISH, fluorescence in situ hybridization; *FLI1*, Fli-1 proto-oncogene; *FUS*, FUS RNA binding protein; M, male; MLPS, myxoid liposarcoma; NA, not available; NGS, next-generation sequencing; NP, not provided; *PDGFB*, platelets-derived growth factor β; SS, synovial sarcoma; *SS18*, synovial sarcoma translocation chromosome 18; *SSX*, synovial sarcoma/X breakpoint; *TFE3*, transcription factor binding to IGHM enhancer 3.

35 STSs diagnosed as follows: alveolar soft-part sarcoma (ASPS) (n=9), Ewing's sarcoma (ES) (n=4), synovial sarcoma (SS) (n=8), dermatofibrosarcoma protuberans (DFSP) (n=9), and myxoid liposarcoma (MLPS) (n=5). IHC using highly specific antibodies was performed on all samples. NGS was successfully performed on 34 of the 35 samples and Sanger sequencing was performed for all 34 samples. Only 12 (35.29%) samples were examined by conventional FISH analysis due to the lack of availability.

Gene fusions identified by NGS

A high sequencing passing rate (100%) was observed with the Ion AmpliSeq™ Custom panels and each qualified run produced an average of 200,000 unique reads. As shown in *Table 2*, the most identified gene fusion was *COL1A1-PDGFB* (n=16) followed by synovial sarcoma translocation chromosome 18 (*SS18*)-synovial sarcoma/X breakpoint family member 1 (*SSX1*) (n=8), and ASPS chromosome region candidate 1 (*ASPSCR1*)-transcription factor for immunoglobulin heavy-chain enhancer 3 (*TFE3*) (n=8). All *SS18-SSX1* fusions occurred between *SS18* exon 10 and *SSX1* exon 6 in the SS samples, while among the *ASPSCR1-TFE3* fusions in eight ASPS specimens, five were exon 7/5 fusions and three were exon 7/6 fusions. Notably, *COL1A1-PDGFB* was not only identified in different STS types, including ASPS (n=1), ES (n=2), SS (n=1), DFSP (n=9), and MLPS (n=3), but also showed much more variant subtypes. The additional gene fusions identified by NGS in ES included Ewing sarcoma breakpoint region 1 gene (*EWSR1*)-ETS transcription factor (*ERG*) exon 7/10 fusion (n=1) and *EWSR1*-Fli-1 proto-oncogene (*FLI1*) exon 7/6 fusion (n=3). We also identified one case each of FUS RNA binding protein (*FUS)-DDIT3* exon 5/2 fusion, exon 7/2 fusion, and exon 8/2 fusion in MLPS. Taken together, all gene fusions were correctly identified by NGS and subsequently further validated.

Concordance between NGS and pathological diagnosis

All the typical gene fusions in common STSs, including ASPS, ES, SS, DFSP, and MLPS, were identified by NGS in our study. ASPS is a rare, malignant STS with poor prognosis that mostly occurs in the extremities in adolescents and young adults (15,16). Its predominant translocation is the fusion of *ASPSCR1* to the *TFE3*, and this was identified in all eight ASPS specimens by NGS.

ES mainly affects the long bones or vertebral regions of young people and children. Approximately 85–90% of patients carry the *EWSR1-FLI1* fusion gene, and 9–14% of patients carry *EWR1-ERG*, both of which encode chimeric transcription factors (17). In our study, one *EWSR1-ERG* and three *EWSR1-FLI1* fusions were detected in four ES samples by NGS.

SS tumors often arises deep in the soft tissue near a joint in the extremity of a young adult patient (18), and are mostly characterized by a fusion between the *SS18* (*SYT*) gene on chromosome 18 and one of the *SSX* genes on the X chromosome, producing *SS18-SSX1*, *SS18-SSX2*, or *SS18-SSX4* chimeric chromatin regulators (15-17,19-22). Our NGS results revealed that all eight SS samples in this research carried the exon 10/6 *SS18-SSX1* fusion.

DFSP is a rare but low-grade malignant skin tumor with frequent local recurrence characterized by the fusion of the *COL1A1* gene on chromosome 17 with the *PDGFB* gene on chromosome 22 (23). COL1A1 up-regulates the expression of platelet-derived growth factor receptor (PDGFR), which acts as an auto-growth or paracrine growth factor. Imatinib mesylate (Gleevec®) is an inhibitor of tyrosine kinases in the PDGFR pathway which has shown a dramatic response in treating patients with metastatic DFSP (24). Different *COL1A1-PDGFB* exon fusion patterns were identified in eight DFSP samples by NGS.

MLPS is composed of univacuolar and multivacuolar lipoblasts embedded in a richly myxoid ground substance, and approximately 30% of MLPS patients develop distant metastases (3). Most MLPS patients show a specific chromosomal translocation that results in the rearrangement of the *FUS* and *DDIT3* genes to encode chimeric transcription factors (25,26). We identified one case each of *FUS-DDIT3* exon 5/2 fusion, exon 7/2 fusion, or exon 8/2 fusion in three MLPS cases.

Analysis of method correlations and agreement

As shown in *Table 2*, all eight of the *COL1A1-PDGFB* FISH positive samples were also identified as *COL1A1-PDGFB* positive by NGS, showing a 100% concordance rate. In addition, NGS identified *COL1A1-PDGFB* fusion in two FISH negative samples, one ES, and one SS sample, suggesting it is more sensitive in detecting this variant. The results of NGS and FISH were also consistent in two SS samples with *SS18-SSX1* exon 10/6 fusion (*Figure 1*) and one MLPS case with *FUS-DDIT3* exon 5/2 fusion (*Figure 2*).

In the other STS samples that were not tested by FISH, Sanger sequencing and NGS were also consistent with detecting gene fusion subtypes. Interestingly, in two ASPS samples with the *ASPSCR1-TFE3* exon 7/5 fusion, TFE3 was also positive for IHC detection, indicating an agreement between IHC, Sanger sequencing, and NGS (*Figure 3*).

Discussion

Based on molecular cytogenetic analysis, STS can be divided into two categories: (I) STS with translocations leading to oncogenic fusion transcripts such as *EWSR1-FLI1* in ES, *FUS-DDT3* in MLPS, and *SS18-SSX* in SS; and (II) STS with specific oncogenic mutations, such as *KIT* and *PDGFRA* mutations in gastrointestinal stromal tumors (1). For this, traditional methods such as FISH, IHC, or Sanger sequencing may be the preferred method to detect a small number of known fusion genes due to the high cost of NGS. However, traditional methods for multi-target analysis of multiple samples may also be costly and time-consuming. The development of the new Ion AmpliSeq™ Custom Panels provides a potential solution to the current limitations. The massively parallel nature of NGS allows a rapid characterization of point mutations, small insertions and deletions. Additionally, NGS can detect chromosome rearrangements of a large set of genes by targeted sequencing of the fusion junctions or by paired-end mapping methods. To evaluate the genetic changes and fusion transcripts in STS, NGS based on poly-A(+) mRNA molecules can increase the capacity to detect gene fusions dramatically. The splicing of non-coding introns that occurs during RNA processing leads to smaller mRNA molecules of the fusion gene compared with the corresponding DNA, which can increase the coverage of the fusion sequence in NGS. Another advantage of NGS is that analysis at the transcript level not only provides information about potential gene fusion sequences, but also about expression variants. In this study, we used Ion AmpliSeq™ Custom panels (IAD187473 and WG_IAD 186692) for sensitive detection of gene fusions with the Ion PGM™ System. This system is integrated with Ion Reporter™ Software v5.0, which includes easy-to-use multi-sample visualization tools, push-button fusion data analysis and classification, and gene expression details. Although several reports have used NGS for molecular profiling of sarcomas (27,28), research on gene fusions in STS is still extremely limited to date. To the best of our knowledge, the application of Ion AmpliSeq™ Custom panels (IAD187473 and WG_IAD 186692) has never been reported and this is the first investigation using this approach to detect structural variants in clinical STS samples.

FISH and RT-PCR-based Sanger sequencing are currently used to detect gene fusion events. However, both these methods present limitations. For example, most FISH assays use break-apart probes to detect whether a certain donor gene has a translocation or rearrangement, but this strategy cannot determine the acceptor genes. Ideally, fusion probes can help determine the specific type of gene fusions. However, some STSs have multiple variant types, and some have a low frequency of fusion events. Using fusion probes to explore all types of gene fusion events would involve a high cost and is not suitable for routine

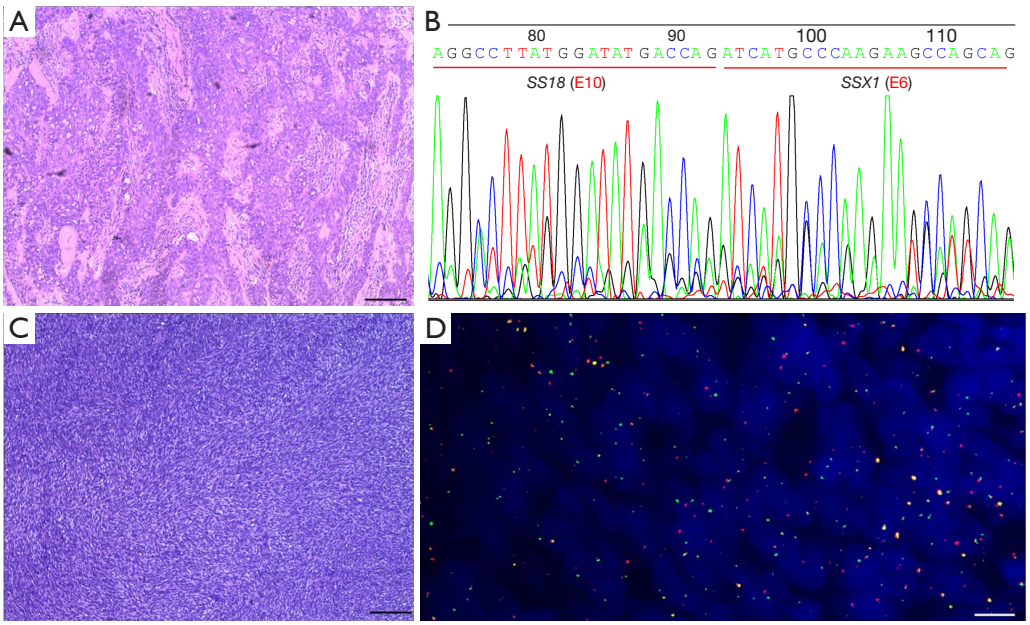

Figure 1 The results of a representative SS case. (A) Morphology of SS cells in case 29. H&E staining was performed on the deparaffinized and ethanol dehydrated 5-μm FFPE slides according to the manufacturer's instruction. The spindle and epithelioid cells were observed in tumor tissues adjacent to the left femoral vein with mild to moderate atypia and pathological mitotic figures. The epithelioid cells are arranged in a pattern resembling a pseudo-adenoid and a sieve. Locally, fissure-like structures are observed resulting from interstitial collagen degeneration, calcification or ossification, and invasion of adjacent fibrous tissues. IHC analysis revealed the presence of AE1/AE3 (epithelial-like area +), vimentin (+), Ki67 (+, 30%), CD34 (–), S100 (–), desmin (–), SMA (–), EMA (epithelial-like area +), BcL-2 (spindle area +), calponin (spindle area +), CD99 (+), and CD117 (individual +). Positive staining for reticulin was observed in interepithelial-like and spindle areas. Scale bar =20 μm. (B) Sanger sequencing of PCR product confirmed an *SS18-SSX1* fusion. (C) A spindle cell tumor was discovered in H&E staining of a left foot biopsy of case 26. The IHC results of AE1/AE3 (–), vimentin (+), CD34 (vascular +), desmin (–), SMA (vascular +), S100 (–), Ki67 (+, local 30%), BcL-2 (+), CD99 (+), EMA (+), and HMB45 (–) were also consistent with the diagnosis of SS. Scale bar =20 μm. (D) FISH revealed *SYT* gene rupture rearrangement, with the 5' *SYT* (18q11) probe labeled with red fluorescence, and the 3' *SYT* probe labeled with green fluorescence. Scale bar =20 μm. FFPE, formalin-fixed paraffin-embedded; FISH, fluorescence in situ hybridization; H&E, hematoxylin and eosin; IHC, immunohistochemistry; SS, synovial sarcoma; *SYT*, synaptotagmin.

clinical practice. RT-PCR-based Sanger sequencing can determine the specific fusion site by DNA sequencing. However, this approach shows problems of low throughput and the detection of only one fusion pattern at a time. More importantly, as these methods are only suitable for detecting specific pre-identified genetic variants and inevitably rely on previous diagnostic assumptions, they cannot meet the purpose of relying on genetic profiling to verify or even correct traditional clinical and pathological diagnosis. NGS is an approach that can overcome these limitations. By allowing the simultaneous analysis of multiple targets and increasing the sequencing depth to achieve ultra-sensitivity, it can not only detect common genetic abnormalities without prior assumptions but also identify uncommon or even new variants.

We compared the applicability of NGS for gene fusion detection with results from FISH and RT-PCR-based Sanger sequencing, and NGS showed superior results. In the 35 STS samples with qualified NGS results, all gene fusions (100%) that are highly specific for pathological diagnosis were accurately identified. NGS also detected three cases of *COL1A1-PDGFB* fusion, which showed negative results in FISH, and several *COL1A1-PDGFB*, *SS-SSX*, and *FUS-DDIT3* fusions that were negative in Sanger sequencing. Small breaks and insertions that cannot be covered by the FISH probe sequences may also cause false negative results of *COL1A1-PDGFB*. The sensitivity of FISH can also be hampered by the low percentage of STS cells carrying the *COL1A1-PDGFB* variants. We also speculate that the low versatility of PCR primers and the low proportion of tumor

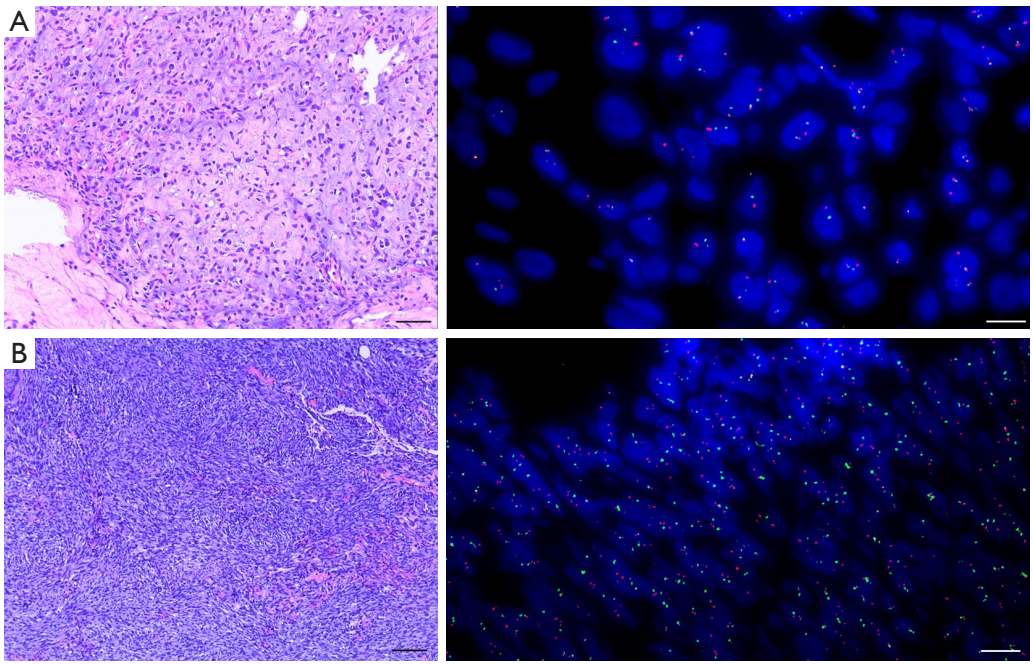

Figure 2 The results of representative MLPS cases. (A) In case 6, FISH indicated a *DDIT3* gene rearrangement in MLPS by the 5' *DDIT3* (12q13) probe labeled with red fluorescence and the 3' *DDIT3* probe labeled with green fluorescence. The lesion on the posterior side of the right thigh was found to be a spindle cell tumor that was nodular and lobulated by H&E staining. Small round cells and slender branched reticular blood vessels can be seen in the mucus matrix, accompanied by local edema and microcystic degeneration. Immature adipose tissue invaded the surrounding striated muscle, accompanied by necrotic calcification. IHC revealed AE1/AE3 (–), vimentin (+), CD34 (vascular +), CD31 (vascular endothelium +), FVIII (vascular endothelium +), S-100 (+), SMA (–), Ki67 (+, 10%), Fli-1 (+), CDK4 (+), and MUC4 (–), consistent with the MLPS diagnosis. Scale bar =20 μm. (B) FISH of case 16 revealed a *COL1A1-PDGFB* fusion in DFSP using the *PDGFB* (22q13) probe labeled with red fluorescence and the *COL1A1* (17q21) probe labeled with green fluorescence. Scale bar =20 μm. *COL1A1*, collagen 1A1; *DDIT3*, DNA damage inducible transcript 3; DFSP, dermatofibrosarcoma protuberans; FISH, fluorescence in situ hybridization; H&E, hematoxylin and eosin; IHC, immunohistochemistry; MLPS, myxoid liposarcoma; MUC4, mucin 4; *PDGFB*, platelets-derived growth factor β; SMA, smooth muscle actin.

cells containing target variants are the main reasons for the false positives of RT-PCR-based Sanger sequencing. For example, the *SS18-SSX4* chimeric variant detected by NGS is a rare case, which is characterized by high breakpoint variability resulting in abnormal transcripts that cannot be detected by conventional methods (23,24). For the sample that was detected by DDIT3 break-apart probes but negative in Sanger sequencing, NGS successfully identified the *FUS-DDIT3* exon 5/2 fusion (29).

In the current era of precision medicine, accurate molecular classification of STS can predict the extent to which patients will benefit from different targeted treatment strategies. Lucchesi *et al.* investigated the role of targeted NGS testing in 584 STS patients and showed that up to 41% of STSs harbored at least one clinically relevant genomic alteration with the potential to influence personalized therapy (30). In the present study, the effectiveness of NGS for detecting *COL1A1-PDGFB* has value beyond diagnosis. For patients with metastatic or unresectable DFSP, NGS findings also expand their chances of choosing imatinib as a targeted therapy (31,32). Genetically, DFSP is characterized in the vast majority of cases by fusion of the *COL1A1-PDGFB* gene, whereas *COL1A1-PDGFB* fusion was also detected in other subtypes of STSs in our study. The promoter and variable part of *COL1A1* gene fused with exon 2 of *PDGFB* gene, resulting in dysregulation of *PDGFB* protein expression (33). At the chromosomal level, gene fusion is caused by the exchange of material between bands 17Q21 (*COL1A1*) and 22Q13 (*PDGFB*). This exchange may be balanced or unbalanced t(17; 22), and may also occur as one or more redundant circular chromosomes. As previously mentioned, *COL1A1-*

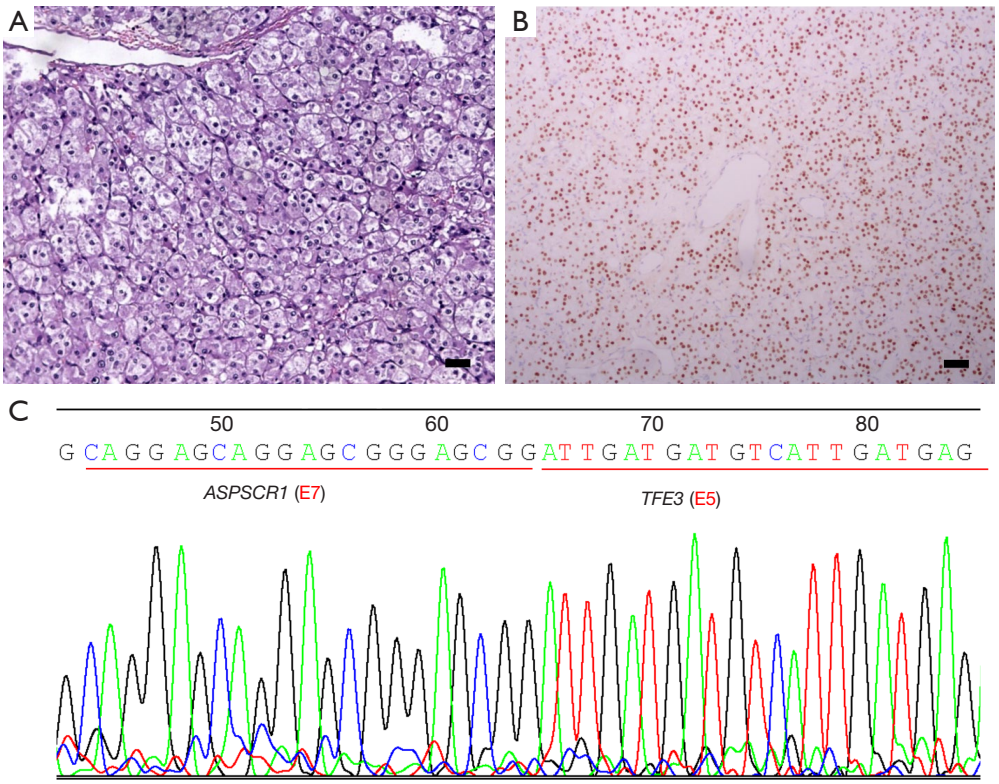

Figure 3 The results of a representative ASPS case. (A) In case 1, H&E staining showed classic morphology of ASPS. Clear cells and a few pale pink stains were observed in the tumor tissue of the right temporal lesion, along with an acinar-like and nest-like distribution, abundant sinusoids, hemorrhage, and necrosis. IHC revealed AE1/AE3 (–), vimentin (–), TFE3 (+), desmin (–), MyoD1(–), SMA (–), EMA (+, local), CD34 (vascular +), S-100 (–), Syn (–), CgA (–), Ki67 (+, 15%), myogenin (–), CD56 (–), HMB45 (–), and Melan-A (–). Positive staining for reticulin was observed, Scale bar =20 μm. (B) IHC for nuclear TFE3 staining demonstrated TFE3 translocation-associated ASPC. Scale bar =20 μm. (C) Sanger sequencing of PCR product confirmed an *ASPSCR1-TFE3* fusion. ASPS, alveolar soft-part sarcoma; *ASPSCR1*, alveolar soft part sarcoma critical region-1; CgA, chromogranin A; EMA, endomysial antibody; H&E, hematoxylin and eosin; HMB45, human melanoma black 45; IHC, immunohistochemistry; SMA, smooth muscle actin; Syn, synapsin; *TFE3*, transcription factor binding to IGHM enhancer 3.

PDGFB fusion is associated with classical translocation or one or more supernumerary ring chromosomes in an age-dependent manner (34). The timing and origin of the repair of translocations and other types of DNA double-strand errors are still not fully understood, but according to cytogenetic data, most tumor-associated translocations leading to pathogenic fusions are due to G0-G1 errors (35). Possibly, the *COL1A1-PDGFB* fusion is only sufficient to promote tumorigenesis in the pediatric setting, while most children and all adults require not only the gene fusion but also an extra copy of the distal 17q and/or /or a distorted ratio between genes centromeric and telomeric to the *PDGFB* locus on chromosome 22. Thus, different types of translocations may occur with equal frequency in all age groups, but only unbalanced translocations have a selective advantage in older patients (36). Several breakpoints have been described for *EWSR1/FLI1* and *EWSR1/ERG* in STSs. The most common events are *EWSR1* exon 7 and *FLI1* exon 6 (defined as type I) or *ERG* exon 6, 7, and 9 (37). Interestingly, a rare pattern of *EWSR1-ERG* exon 7/10 fusion was identified by NGS. Lin *et al.* found that type 1 *EWS-FLI1* fusion, which encodes a less active chimeric transcription factor, was associated with a significantly better prognosis than the other fusion types (38). However, more evidence is required to clarify how the *EWSR1-ERG* exon 7/10 fusion is correlated with patient prognosis. Another rare case that carried *SS18-SSX1* and *SS18-SSX4* fusion was detected by NGS but

not by Sanger sequencing. Kawai *et al.* first described relationship between the *SYT-SSX* fusion transcript and the histologic subtype and clinical behaviors of SS (39). In addition, Saito *et al.* proposed that almost all biphasic SS harbors the *SYT-SSX1* fusion gene (40). This gene is a potent oncogene that plays a key role in the pathogenesis of SS. Patients with SS have a poor prognosis (10-year survival rate: 10–30%) (41). Moreover, Ladanyi *et al.* found STS patients with *SS18-SSX2* tumors had a better prognosis than those with *SS18-SSX1* tumors (42). However, our sample size was too limited to draw the conclusion that patient carrying both *SS18-SSX1* and *SS18-SSX4* had a significantly different outcome. A recent report from the European Paediatric Soft Tissue Sarcoma Group (EpSSG) examined the results of fusion status in 103 patients with alveolar rhabdomyosarcoma (RMS) with N1 disease. Results showed that patients with a positive *FOXO1* fusion gene had a poorer prognosis than patients with a negative fusion gene and affected 5-year event-free survival (EFS) in these patients (43%) (43). In addition, some molecular genetic markers for STSs have been reported. Greither *et al.* found low expression of piwi like RNA-mediated gene silencing 2 (*PIWIL2*) mRNA was significantly associated with poor prognosis (44). High MDM4S mRNA expression was associated with short treatment-free survival, and its overexpression was significantly associated with poor prognosis (45,46).

In conclusion, this study provides evidence for the diagnostic use of Ion AmpliSeq™ Custom panels (IAD187473 and WG_IAD 186692) to detect gene fusion in STS. We demonstrated the superior results of these panels in accuracy and sensitivity compared with traditional methods. NGS represents a promising clinical tool for STS diagnosis with additional advantages, including the acquisition of prognostic and therapeutic predictive information in a single assay.

Acknowledgments

We thank Shanghai Tongshu Biotechnology Co., Ltd. for technical support.

Funding: The work was supported by a grant from the Natural Science Foundation of Shanxi Province (No. 201901D211498) and the Youth Science foundation of Second Hospital of Shanxi Medical University (No. 201902-1).

Footnote

Reporting Checklist: The authors have completed the MDAR reporting checklist. Available at https://tcr.amegroups.com/article/view/10.21037/tcr-22-70/rc

Data Sharing Statement: Available at https://tcr.amegroups.com/article/view/10.21037/tcr-22-70/dss

Conflicts of Interest: All authors have completed the ICMJE uniform disclosure form (available at https://tcr.amegroups.com/article/view/10.21037/tcr-22-70/coif). All authors report that the study received technical support from Shanghai Tongshu Biotechnology Co., Ltd. The authors have no other conflicts of interest to declare.

Ethical Statement: The authors are accountable for all aspects of the work in ensuring that questions related to the accuracy or integrity of any part of the work are appropriately investigated and resolved. The study was conducted in accordance with the Declaration of Helsinki (as revised in 2013). The study was approved by the ethics committees of the Second Hospital of Shanxi Medical University [(2021)YX No.019] and informed consent was taken from all the patients.

References

1. Bridge JA. The role of cytogenetics and molecular diagnostics in the diagnosis of soft-tissue tumors. Mod Pathol 2014;27 Suppl 1:S80-97.
2. Fletcher CDM, Bridge JA, Hogendoorn PCW, et al. editors. WHO Classification of tumours of soft tissue and bone. 4th edition. WHO, 2013.
3. Pillozzi S, Bernini A, Palchetti I, et al. Soft Tissue Sarcoma: An Insight on Biomarkers at Molecular, Metabolic and

Cellular Level. Cancers (Basel) 2021;13:3044.
4. Peinado H, Zhang H, Matei IR, et al. Pre-metastatic niches: organ-specific homes for metastases. Nat Rev Cancer 2017;17:302-17.
5. Helman LJ, Meltzer P. Mechanisms of sarcoma development. Nat Rev Cancer 2003;3:685-94.
6. Taylor BS, Barretina J, Maki RG, et al. Advances in sarcoma genomics and new therapeutic targets. Nat Rev Cancer 2011;11:541-57.
7. Drilon A, Laetsch TW, Kummar S, et al. Efficacy of Larotrectinib in TRK Fusion-Positive Cancers in Adults and Children. N Engl J Med 2018;378:731-9.
8. Sorensen PH, Lynch JC, Qualman SJ, et al. PAX3-FKHR and PAX7-FKHR gene fusions are prognostic indicators in alveolar rhabdomyosarcoma: a report from the children's oncology group. J Clin Oncol 2002;20:2672-9.
9. Debiec-Rychter M, Marynen P, Hagemeijer A, et al. ALK-ATIC fusion in urinary bladder inflammatory myofibroblastic tumor. Genes Chromosomes Cancer 2003;38:187-90.
10. Chen ST, Lee JC. An inflammatory myofibroblastic tumor in liver with ALK and RANBP2 gene rearrangement: combination of distinct morphologic, immunohistochemical, and genetic features. Hum Pathol 2008;39:1854-8.
11. Barthelmeß S, Geddert H, Boltze C, et al. Solitary fibrous tumors/hemangiopericytomas with different variants of the NAB2-STAT6 gene fusion are characterized by specific histomorphology and distinct clinicopathological features. Am J Pathol 2014;184:1209-18.
12. Overman MJ, McDermott R, Leach JL, et al. Nivolumab in patients with metastatic DNA mismatch repair-deficient or microsatellite instability-high colorectal cancer (CheckMate 142): an open-label, multicentre, phase 2 study. Lancet Oncol 2017;18:1182-91.
13. van Gestel YR, de Hingh IH, van Herk-Sukel MP, et al. Patterns of metachronous metastases after curative treatment of colorectal cancer. Cancer Epidemiol 2014;38:448-54.
14. Willeke F, Mechtersheimer G, Schwarzbach M, et al. Detection of SYT-SSX1/2 fusion transcripts by reverse transcriptase-polymerase chain reaction (RT-PCR) is a valuable diagnostic tool in synovial sarcoma. Eur J Cancer 1998;34:2087-93.
15. Barr FG, Qualman SJ, Macris MH, et al. Genetic heterogeneity in the alveolar rhabdomyosarcoma subset without typical gene fusions. Cancer Res 2002;62:4704-10.
16. Liu J, Guzman MA, Pezanowski D, et al. FOXO1-FGFR1 fusion and amplification in a solid variant of alveolar rhabdomyosarcoma. Mod Pathol 2011;24:1327-35.
17. Baldauf MC, Gerke JS, Orth MF, et al. Are EWSR1-NFATc2-positive sarcomas really Ewing sarcomas? Mod Pathol 2018;31:997-9.
18. Panagopoulos I, Mertens F, Isaksson M, et al. Clinical impact of molecular and cytogenetic findings in synovial sarcoma. Genes Chromosomes Cancer 2001;31:362-72.
19. Mosquera JM, Sboner A, Zhang L, et al. Recurrent NCOA2 gene rearrangements in congenital/infantile spindle cell rhabdomyosarcoma. Genes Chromosomes Cancer 2013;52:538-50.
20. Dahlén A, Fletcher CD, Mertens F, et al. Activation of the GLI oncogene through fusion with the beta-actin gene (ACTB) in a group of distinctive pericytic neoplasms: pericytoma with t(7;12). Am J Pathol 2004;164:1645-53.
21. Butrynski JE, D'Adamo DR, Hornick JL, et al. Crizotinib in ALK-rearranged inflammatory myofibroblastic tumor. N Engl J Med 2010;363:1727-33.
22. Heinrich MC, Corless CL, Demetri GD, et al. Kinase mutations and imatinib response in patients with metastatic gastrointestinal stromal tumor. J Clin Oncol 2003;21:4342-9.
23. Skytting B, Nilsson G, Brodin B, et al. A novel fusion gene, SYT-SSX4, in synovial sarcoma. J Natl Cancer Inst 1999;91:974-5.
24. Brodin B, Haslam K, Yang K, et al. Cloning and characterization of spliced fusion transcript variants of synovial sarcoma: SYT/SSX4, SYT/SSX4v, and SYT/SSX2v. Possible regulatory role of the fusion gene product in wild type SYT expression. Gene 2001;268:173-82.
25. Urbini M, Astolfi A, Pantaleo MA, et al. HSPA8 as a novel fusion partner of NR4A3 in extraskeletal myxoid chondrosarcoma. Genes Chromosomes Cancer 2017;56:582-6.
26. Sunitsch S, Gilg MM, Kashofer K, et al. Detection of GNAS mutations in intramuscular / cellular myxomas as diagnostic tool in the classification of myxoid soft tissue tumors. Diagn Pathol 2018;13:52.
27. Jour G, Scarborough JD, Jones RL, et al. Molecular profiling of soft tissue sarcomas using next-generation sequencing: a pilot study toward precision therapeutics. Hum Pathol 2014;45:1563-71.
28. Groisberg R, Roszik J, Conley A, et al. The Role of Next-Generation Sequencing in Sarcomas: Evolution From Light Microscope to Molecular Microscope. Curr Oncol Rep 2017;19:78.
29. Powers MP, Wang WL, Hernandez VS, et al. Detection

of myxoid liposarcoma-associated FUS-DDIT3 rearrangement variants including a newly identified breakpoint using an optimized RT-PCR assay. Mod Pathol 2010;23:1307-15.
30. Lucchesi C, Khalifa E, Laizet Y, et al. Targetable Alterations in Adult Patients With Soft-Tissue Sarcomas: Insights for Personalized Therapy. JAMA Oncol 2018;4:1398-404.
31. Noujaim J, Thway K, Fisher C, et al. Dermatofibrosarcoma protuberans: from translocation to targeted therapy. Cancer Biol Med 2015;12:375-84.
32. Labropoulos SV, Razis ED. Imatinib in the treatment of dermatofibrosarcoma protuberans. Biologics 2007;1:347-53.
33. Simon MP, Pedeutour F, Sirvent N, et al. Deregulation of the platelet-derived growth factor B-chain gene via fusion with collagen gene COL1A1 in dermatofibrosarcoma protuberans and giant-cell fibroblastoma. Nat Genet 1997;15:95-8.
34. Sirvent N, Maire G, Pedeutour F. Genetics of dermatofibrosarcoma protuberans family of tumors: from ring chromosomes to tyrosine kinase inhibitor treatment. Genes Chromosomes Cancer 2003;37:1-19.
35. Biehs R, Steinlage M, Barton O, et al. DNA Double-Strand Break Resection Occurs during Non-homologous End Joining in G1 but Is Distinct from Resection during Homologous Recombination. Mol Cell 2017;65:671-684.e5.
36. Köster J, Arbajian E, Viklund B, et al. Genomic and transcriptomic features of dermatofibrosarcoma protuberans: Unusual chromosomal origin of the COL1A1-PDGFB fusion gene and synergistic effects of amplified regions in tumor development. Cancer Genet 2020;241:34-41.
37. Cantile M, Marra L, Franco R, et al. Molecular detection and targeting of EWSR1 fusion transcripts in soft tissue tumors. Med Oncol 2013;30:412.
38. Lin PP, Brody RI, Hamelin AC, et al. Differential transactivation by alternative EWS-FLI1 fusion proteins correlates with clinical heterogeneity in Ewing's sarcoma. Cancer Res 1999;59:1428-32.
39. Kawai A, Woodruff J, Healey JH, et al. SYT-SSX gene fusion as a determinant of morphology and prognosis in synovial sarcoma. N Engl J Med 1998;338:153-60.
40. Saito T. The SYT-SSX fusion protein and histological epithelial differentiation in synovial sarcoma: relationship with extracellular matrix remodeling. Int J Clin Exp Pathol 2013;6:2272-9.
41. Barham W, Frump AL, Sherrill TP, et al. Targeting the Wnt pathway in synovial sarcoma models. Cancer Discov 2013;3:1286-301.
42. Ladanyi M, Antonescu CR, Leung DH, et al. Impact of SYT-SSX fusion type on the clinical behavior of synovial sarcoma: a multi-institutional retrospective study of 243 patients. Cancer Res 2002;62:135-40.
43. Brennan B, Zanetti I, Orbach D, et al. Alveolar soft part sarcoma in children and adolescents: The European Paediatric Soft Tissue Sarcoma study group prospective trial (EpSSG NRSTS 2005). Pediatr Blood Cancer 2018.
44. Greither T, Koser F, Kappler M, et al. Expression of human Piwi-like genes is associated with prognosis for soft tissue sarcoma patients. BMC Cancer 2012;12:272.
45. Liu L, Fan L, Fang C, et al. S-MDM4 mRNA overexpression indicates a poor prognosis and marks a potential therapeutic target in chronic lymphocytic leukemia. Cancer Sci 2012;103:2056-63.
46. Lenos K, Grawenda AM, Lodder K, et al. Alternate splicing of the p53 inhibitor HDMX offers a superior prognostic biomarker than p53 mutation in human cancer. Cancer Res 2012;72:4074-84.

(English Language Editor: B. Draper)

Cite this article as: Wei R, Gao F, Zeng Z, Gui Z, Shang Y, Shen N, Wang Z, Han W, Shen H, Li X, E L, Ma W, Wang C. Molecular profiling of gene fusions in soft tissue sarcomas by Ion AmpliSeq™: a study of 35 cases. Transl Cancer Res 2022;11(3):488-499. doi: 10.21037/tcr-22-70

